Distributed control for output consensus of multi-satellite systems

M. Araújo * **P. Oliveira** **

* *Instituto de Engenharia Mecânica - IDMEC, 1049-001 Lisboa, Portugal (e-mail: miguel.barreiro.de.araujo@tecnico.ulisboa.pt).*
** *Instituto de Engenharia Mecânica - IDMEC, 1049-001 Lisboa, Portugal (e-mail: paulo.j.oliveira@tecnico.ulisboa.pt).*

Abstract: In this paper, a non-linear output feedback control strategy is employed to design a distributed formation controller for a constellation of satellites, in order to achieve a coordinated action on Earth observation. The formation controller uses notions of graph algebra and consensus theory. A stable non-linear control law is proposed to ensure consensus on a function of the states, while actuating in the second derivative of the states, using backstepping techniques. The control law uses the full dynamics of the satellites and is proven to achieve a bounded output for perturbations with bounded time derivative. The control law is further adapted to the satellite's dynamics, described through Euler angles. Satellites with different orbits are proven to observe points in the surface of the Earth with the desired coordination.

Keywords: Distributed nonlinear control, Consensus, Output feedback control, Nonlinear cooperative control, Satellites, Multi-agent systems

1. INTRODUCTION

With the continuous development of the technology of autonomous vehicles, multi-vehicle applications are increasingly more desirable and relevant in various domains, since complex tasks may be accomplished using multiple simpler vehicles rather than a single complex one. It comes to no surprise that the study of advanced control methods for these kinds of problems spark a peculiar interest, since the dynamically decoupled vehicles, with limited information about the whole group, must act coordinated. In satellite applications, the relevance heightens with the increasing pursuit of satellite constellations and the cooperative burden that they share. Global Positioning Systems and Satellite Communication Networks, such as Starlink, are but a few examples of satellite constellations that can only function with the cooperation of vehicles. Thus, coordination of multiple satellite systems, namely in attitude, becomes a necessity for a great number of possible applications.

In Fax and Murray (2004), Olfati-Saber and Murray (2004) and Olfati-Saber et al. (2007), ideas from graph theory were introduced in control theory to develop a criterion of stability in consensus problems, both in linear and non-linear settings for various types of information flow. These ideas are very useful in the design of global controllers for multi-agent systems, focusing only on the interactions between vehicles rather than their individual behavior.

Multiple works have explored the path of control for multi-satellite systems, such as Lawton and Beard (2002) and Ren (2002), where quaternions were used to design a distributed control law that allowed synchronized rotations and attitude alignment. In Wu et al. (2020a) and Wu et al. (2020b) a characteristic model of the vehicles was introduced in order to achieve the same goal.

Other authors have worked on solutions for distributed multi-satellite control problems over limited environments. For instance, in Abdessameud and Tayebi (2008), an attitude control solution was devised in the absence of angular velocity measurements and in Ziyang et al. (2010) the same was achieved in an environment with time delays in the communications between satellites and with switching communication topologies.

However all these works focus on consensus around the state but, in applications such as Earth observation, for multi-satellite systems to work accordingly, the consensus should not be around the attitude of the individual satellites (the state), but rather on where the satellites are pointing to which is a function of said state. Based on the different positions of the satellites at a given time, it is reasonable to think that, in order to look at a certain point, each satellite must have a different orientation than another one from the same group.

This is the problem that will be addressed in this paper. The proposition is to devise a non-linear distributed controller for a multi-satellite system in order for them to reach consensus around a possible output, considering the full dynamics of these systems. While these tools are presented in a general form in order for them to be applied in multiple cases, in this article, they will be applied to the particular case of Earth observation. The main idea is to increase the field of view of an image while maintaining its high resolution by using the cameras of the multiple satellites in coordination, following similar works on sensor fusion of satellites with limited capabilities, such as in Alvarez and Walls (2016). However, the satellites needn't

be equal nor have sufficiently significant orbits. As it will be presented, the proposed solution for distributed control is independent from the design of individual controllers or specific dynamics for each satellite. The only requirement is that they have the capabilities to receive and transmit information to neighbouring satellites.

This paper is organized as follows: section 2 introduces the satellite kinematic and dynamic equations, as well as the problem statement and objective. Section 3 presents the necessary notions and results on consensus theory to develop the distributed controller. Section 4 details the design of the distributed controller, in order to achieve output tracking and evaluates its performance from perturbations on the output. In section 5, a simulation is presented in order to experimentally assess the performance of the control law and its behaviour when facing perturbations. Finally, in section 6, all the results are summed up in a conclusion, just as some ideas for future topics of investigation.

NOTATION

In this paper, vectors will be denoted by bold lower-case letters (e.g. $\boldsymbol{u}$, $\boldsymbol{x}$), matrices will be represented by bold upper-case letters (e.g. $\boldsymbol{R}, \boldsymbol{L}$) and the i-th element of a vector is denoted $\boldsymbol{x}_i$. The symbol $\mathbf{0}$ stands for a matrix full of zeros, with appropriate dimensions, and $\boldsymbol{I}_n$ represents an $n \times n$ identity matrix. The time derivative of a quantity s is denoted by $\dot{s}$. The usage of $[\boldsymbol{v}\times]$ defines the skew-symmetric of a generic vector $\boldsymbol{v} \in \mathbb{R}^3$ in matrix form as

$$[\boldsymbol{v}\times] = \begin{bmatrix} 0 & -\boldsymbol{v}_3 & \boldsymbol{v}_2 \\ \boldsymbol{v}_3 & 0 & -\boldsymbol{v}_1 \\ -\boldsymbol{v}_2 & \boldsymbol{v}_1 & 0 \end{bmatrix}.$$

An inertial frame of reference, assumed for simplicity to be Earth Centered Inertial, is denoted by $\{I\}$ and $\{B\}$ represents the vehicle's body frame. Frame $\{S\}$ will also be used to locate the points on the surface of the Earth to where the satellites are pointing, and the origin will be located at the equator and at the prime meridian. The X axis will be aligned with the equator, pointing to an increase of longitude, and the Y axis will be aligned with the prime meridian, pointing to an increase of latitude.

Finally, the $\otimes$ symbol will be used to write the Kronecker product between matrices and, for a succession of k square matrices $\boldsymbol{A}_i \in \mathbb{R}^{n\times n}$, with $i \in \{1, ..., k\}$, $\hat{\boldsymbol{A}} \in \mathbb{R}^{kn\times kn}$ will be defined as

$$\hat{\boldsymbol{A}} = \begin{bmatrix} \boldsymbol{A}_1 & \dots & \mathbf{0} \\ \vdots & \ddots & \vdots \\ \mathbf{0} & \dots & \boldsymbol{A}_k \end{bmatrix}.$$

2. PROBLEM FORMULATION

2.1 Satellite Dynamics and Kinematics

Consider the satellite vehicle sketch represented in Fig. 1. It is able to actuate in all three axes with a given torque. Let the vehicle's body frame be located at its centre of mass. The differential equations that, respectively, describe the attitude kinematics and dynamics are defined as

$$\dot{\boldsymbol{\lambda}} = \boldsymbol{\Xi}\boldsymbol{\omega}, \tag{1}$$

$$\dot{\boldsymbol{\omega}} = -\boldsymbol{J}^{-1}[\boldsymbol{\omega}\times]\boldsymbol{J}\boldsymbol{\omega} + \boldsymbol{J}^{-1}\boldsymbol{\tau}, \tag{2}$$

where $\boldsymbol{J} \in \mathbb{R}^{3\times3}$ is the inertia matrix with respect to $\{B\}$, $\boldsymbol{\lambda} = [\phi\ \theta\ \psi]^T \in \mathbb{R}^3$ is the vector of the intrinsic Euler angles of basic rotations from $\{I\}$ to $\{B\}$, following the Euler sequence Z-Y-Z, $\boldsymbol{\omega} \in \mathbb{R}^3$ is the angular velocity relative to $\{I\}$, expressed in $\{B\}$, $\boldsymbol{\tau} \in \mathbb{R}^3$ is the total generated torque, expressed in $\{B\}$, and

$$\boldsymbol{\Xi} = \begin{bmatrix} \sin\psi(\sin\theta)^{-1} & \cos\psi(\sin\theta)^{-1} & 0 \\ \cos\psi & -\sin\psi & 0 \\ -\sin\psi\sec\theta & -\cos\psi\sec\theta & 1 \end{bmatrix}. \tag{3}$$

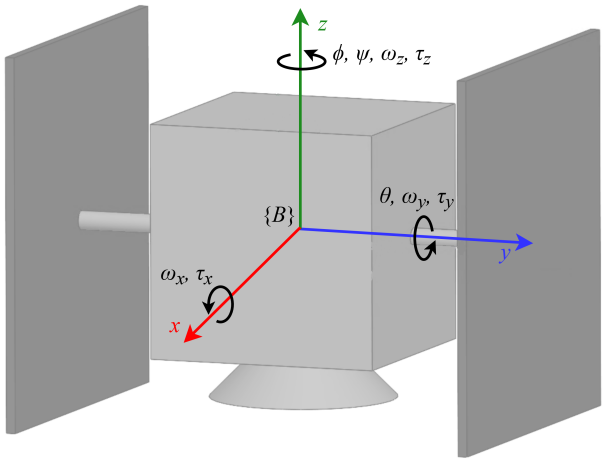

Fig. 1. Diagram of a satellite

Each satellite will observe a point in the Earth as is shown in Fig. 2. The cartesian coordinates of the observed point may be obtained from the state of the vehicle, resulting in the following output equations,

$$\boldsymbol{y} = \begin{bmatrix} h\tan\theta\cos\phi + p_x \\ h\tan\theta\sin\phi + p_y \\ \psi \end{bmatrix}, \tag{4}$$

where p_x and p_y are the coordinates of the point directly below the satellite in the $\{S\}$ frame. Note that the last rotation, ψ, is not required to achieve the proposed goal. However, instead of considering it as a special state, it will be easier to include it in the vehicle's output.

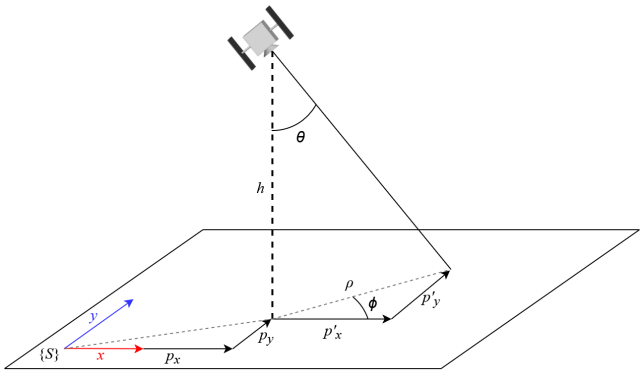

Fig. 2. Diagram of the observation performed by the satellite

2.2 Problem formulation

Consider a set of n different satellites, each with individual kinematics and dynamics described in Eqs. (1) and (2), respectively. Suppose that each satellite is able to measure the relative output to a subset of other vehicles, effectively establishing an information graph $G = (\mathcal{V}, \mathcal{E}, \boldsymbol{\mathcal{A}})$. Here, $\mathcal{V}$ is the set of vertices v_i in the graph (the set of satellites) and $\mathcal{E}$ is the set of edges (v_i, v_j) (connection from satellite i to satellite j). Lastly, let $a_{ij} \in \mathbb{R}_{\geq 0}$ denote the weight of the edge (v_i, v_j) and define $\boldsymbol{\mathcal{A}} = [a_{ij}]$ as the adjacency matrix of the graph. Without loss of generality, it is assumed that the information graph does not contain any self-loops, that is, $a_{ii} = 0,\ i \in \{1, \ldots, n\}$.

Facing a reference signal limited to only a subset of satellites, the objective is to design a distributed control solution that allows the constellation to act in coordination to observe the Earth. For this, assume that each satellite i has a sensor set that is able to know, in real-time and with negligible uncertainty, its attitude $\boldsymbol{\lambda}_i$, its angular velocity $\boldsymbol{\omega}_i$ and the relative output of satellite j, $(\boldsymbol{y}_j - \boldsymbol{y}_i)$. The latter may be obtained by measure inter-communication in the constellation and the former by an Inertial Measurement Unit. Suppose, as well, that each satellite is able to receive information about its velocity relative to $\{S\}$, that is, its planar velocity relative to the motion of the Earth in the equator.

Low Earth Orbits will be considered since the heights are small enough for the surface of the Earth to be approximately flat, making $\{S\}$ a 2D frame. With this assumption, the velocity of the satellites will be considered to have an approximate constant direction.

3. CONSENSUS THEORY

Consider an algebraic directed graph $G_x = (\mathcal{V}, \mathcal{E}, \boldsymbol{\mathcal{A}}, \boldsymbol{x})$ consisting of n nodes, with $\boldsymbol{x}_i \in \mathbb{R},\ i \in \{1, ..., n\}$, denoting the value of node v_i. It is said that the nodes reach a consensus when $\boldsymbol{x}_i = \boldsymbol{x}_j$, for all $i \neq j$.

Define the out-degree of node v_i as

$$\deg_{out}(v_i) = \sum_{j=1}^{n} a_{ij}. \tag{5}$$

The *degree matrix* $\boldsymbol{\Delta} = [\Delta_{ij}]$ is constructed by concatenating the values of the out-degrees of each node in the main diagonal, with $\Delta_{ii} = \deg_{out}(v_i)$ and $\Delta_{ij} = 0,\ \forall i \neq j$. It is possible to define the *Laplacian matrix* associated with G_x as

$$\boldsymbol{L} = \boldsymbol{\Delta} - \boldsymbol{\mathcal{A}}. \tag{6}$$

Remark 1. By construction, all the elements of each row of $\boldsymbol{L}$ sum to zero. Therefore, $\boldsymbol{L}$ has a zero eigenvalue corresponding to the eigenvector $\boldsymbol{w} = [1\ \ldots\ 1]^T$. In other words, the rank of $\boldsymbol{L}$ is lower than n.

A graph is said to be *strongly connected* if and only if every pair of nodes in the graph can be connected via a path that respects the orientation of the edges. In Olfati-Saber and Murray (2004), a very important conclusion is proven in the case of strongly connected graphs.

Theorem 2. Let $G = (\mathcal{V}, \mathcal{E}, \boldsymbol{\mathcal{A}})$ be a weighted directed graph with Laplacian $\boldsymbol{L}$. Then $\text{rank}(\boldsymbol{L}) = n - 1$ if and only if G is strongly connected.

Another important theorem proven in Olfati-Saber and Murray (2004), based on the Geršgorin disk theorem, is also presented.

Theorem 3. Let $G = (\mathcal{V}, \mathcal{E}, \boldsymbol{\mathcal{A}})$ be a weighted directed graph with Laplacian $\boldsymbol{L}$. Let $d_{max}(G) = \max_i \deg_{out}(v_i)$, with $i \in \{1, ..., n\}$. Then all the eigenvalues of $\boldsymbol{L}$ are located in the following disk

$$D(G) = \{z \in \mathbb{C} : |z - d_{max}(G)| \leq d_{max}(G)\}. \tag{7}$$

In this particular application, knowing that each node will represent a satellite, we may view each value as the corresponding satellite's attitude. As a starting point, it is interesting to study the type of dynamic systems described by

$$\begin{cases} \dot{\boldsymbol{x}}_i = \boldsymbol{u}_i \\ \boldsymbol{y}_i = \boldsymbol{f}_i(\boldsymbol{x}_i) + \boldsymbol{g}_i(t) + \boldsymbol{h}_i(t) \end{cases}, \tag{8}$$

where $\boldsymbol{f}_i(\boldsymbol{x}_i)$ refers to the output component fully dependent on the state of the node, $\boldsymbol{g}_i(t)$ is a time dependent component assumed to be known and $\boldsymbol{h}_i(t)$ is an unknown time dependent component. In the application treated in this paper, $\boldsymbol{g}_i(t)$ will represent the effect of the position of the satellites in the output and $\boldsymbol{h}_i(t)$ may represent any perturbative terms present in the model, such as model mismatches or errors that come from the approximations used. Neglecting, for now, the perturbative term, it is possible to write a control law that allows the nodes to reach a consensus around the output.

Theorem 4. Consider a strongly connected algebraic graph $G_x = (\mathcal{V}, \mathcal{E}, \boldsymbol{\mathcal{A}}, \boldsymbol{x})$ with n nodes and a corresponding Laplacian matrix $\boldsymbol{L}$. Let each value $\boldsymbol{x}_i \in \mathbb{R}^m$, with $i \in \{1, ..., n\}$ be defined by the dynamics

$$\begin{cases} \dot{\boldsymbol{x}}_i = \boldsymbol{u}_i \\ \boldsymbol{y}_i = \boldsymbol{f}_i(\boldsymbol{x}_i) + \boldsymbol{g}_i(t) \end{cases}, \tag{9}$$

where $\boldsymbol{u}_i \in \mathbb{R}^m$ is the input of node i and $\boldsymbol{y}_i \in \mathbb{R}^m$ is the output, with $\boldsymbol{f}_i : \mathbb{R}^m \to \mathbb{R}^m$ and $\boldsymbol{g}_i : \mathbb{R} \to \mathbb{R}^m$. Let $\boldsymbol{D}_{f_i} \in \mathbb{R}^{m \times m}$ denote the derivative of $\boldsymbol{f}_i$, $\boldsymbol{u} = [\boldsymbol{u}_1^T\ ...\ \boldsymbol{u}_n^T]^T$, $\boldsymbol{y} = [\boldsymbol{y}_1^T\ ...\ \boldsymbol{y}_n^T]^T$, $\boldsymbol{x} = [\boldsymbol{x}_1^T\ ...\ \boldsymbol{x}_n^T]^T$ and $\boldsymbol{g} = [\boldsymbol{g}_1^T\ ...\ \boldsymbol{g}_n^T]^T$. Assuming that $\boldsymbol{g}(t)$ is a known signal, the control law

$$\boldsymbol{u} = -\hat{\boldsymbol{D}}_f^{-1}(\boldsymbol{L} \otimes \boldsymbol{I}_m)\boldsymbol{y} - \hat{\boldsymbol{D}}_f^{-1}\dot{\boldsymbol{g}}(t) \tag{10}$$

is stable in the domain of $\boldsymbol{f}$ where the derivative is invertible and the outputs of the nodes converge to a common value.

Proof. Consider the candidate Lyapunov function $V = \frac{1}{2}\boldsymbol{y}^T\boldsymbol{y}$. Taking the derivative,

$$\dot{V} = \boldsymbol{y}^T(\hat{\boldsymbol{D}}_f\dot{\boldsymbol{x}} + \dot{\boldsymbol{g}}(t)) = \boldsymbol{y}^T(\hat{\boldsymbol{D}}_f\boldsymbol{u} + \dot{\boldsymbol{g}}(t)). \tag{11}$$

Applying the control law (10), the expression becomes

$$\dot{V} = \boldsymbol{y}^T(\boldsymbol{L} \otimes \boldsymbol{I}_m)\boldsymbol{y} \leq 0, \forall \boldsymbol{y} \in \mathbb{R}^{mn}. \tag{12}$$

It is proven that V is a valid Lyapunov function, which means that the system is stable. Furthermore, the matrix $\boldsymbol{L} \otimes \boldsymbol{I}_m$ shares the same eigenvalues as $\boldsymbol{L}$ but each with algebraic multiplicity equal to m. For each eigenvalue, the corresponding eigenvectors are $\boldsymbol{v} \otimes \boldsymbol{e}_j$, where $\boldsymbol{v}$ are the eigenvectors of $\boldsymbol{L}$ and $\boldsymbol{e}_j$ are unit $m \times 1$ vectors with a 1 in the j-th position, with $j \in \{1, ..., m\}$. Since $[1\ ...\ 1]^T$ is the only eigenvector of $\boldsymbol{L}$ associated with the null eigenvalue, it is shown that $\dot{V}$ is zero when the nodes reach a consensus around every component of their output, confirming the statement that the system converges to a common value.

The system treated until now isn't, however, quite descriptive of the system that is addressed in section 2. One may see, from the vehicle dynamics in (1)-(2), that the input will act, indirectly, on the second derivative of the Euler angles, which in turn affect the output. Thus, the dynamics of the values of nodes resemble a double integrator rather than a single integrator. As such, the control law must be modified to consider this situation. This is achieved in the following theorem using backstepping techniques, as described in Khalil (2001).

Theorem 5. Consider a strongly connected algebraic graph $G_x = (\mathcal{V}, \mathcal{E}, \boldsymbol{\mathcal{A}}, \boldsymbol{x})$ with n nodes and a corresponding Laplacian matrix $\boldsymbol{L}$. Let each value $\boldsymbol{x}_i \in \mathbb{R}^m$, with $i \in \{1, ..., n\}$ be defined by the dynamics

$$\begin{cases} \dot{\boldsymbol{x}}_i = \boldsymbol{w}_i \\ \dot{\boldsymbol{w}}_i = \boldsymbol{u}_i \\ \boldsymbol{y}_i = \boldsymbol{f}_i(\boldsymbol{x}_i) + \boldsymbol{g}_i(t) \end{cases}, \tag{13}$$

where $\boldsymbol{u}_i \in \mathbb{R}^m$ is the input of node i and $\boldsymbol{y}_i \in \mathbb{R}^m$ is the output, with $\boldsymbol{f}_i : \mathbb{R}^m \to \mathbb{R}^m$ and $\boldsymbol{g}_i : \mathbb{R} \to \mathbb{R}^m$. Let $\boldsymbol{D}_{f_i} \in \mathbb{R}^{m\times m}$ denote the derivative of $\boldsymbol{f}_i$, $\boldsymbol{u} = [\boldsymbol{u}_1^T \ ... \ \boldsymbol{u}_n^T]^T$, $\boldsymbol{y} = [\boldsymbol{y}_1^T \ ... \ \boldsymbol{y}_n^T]^T$ and $\boldsymbol{x} = [\boldsymbol{x}_1^T \ ... \ \boldsymbol{x}_n^T]^T$. Let

$$\boldsymbol{\xi}(t, \boldsymbol{y}) = -\hat{\boldsymbol{D}}_f^{-1}(\boldsymbol{L} \otimes \boldsymbol{I}_m)\boldsymbol{y} - \hat{\boldsymbol{D}}_f^{-1}\dot{\boldsymbol{g}}(t) \tag{14}$$

denote the control law obtained in theorem 4. The control law

$$\boldsymbol{u} = -\hat{\boldsymbol{D}}_f^T\boldsymbol{y} + \dot{\boldsymbol{\xi}}(t, \boldsymbol{y}) - \hat{\boldsymbol{K}}(\dot{\boldsymbol{x}} - \boldsymbol{\xi}(t, \boldsymbol{y})) \tag{15}$$

is stable in the domain of $\boldsymbol{f}$ where the derivative is invertible and for $\hat{\boldsymbol{K}} > 0$.

Proof. Making the derivative of the output equations leads to the following system,

$$\begin{cases} \dot{\boldsymbol{y}} = \hat{\boldsymbol{D}}_f\boldsymbol{w} + \dot{\boldsymbol{g}}(t) \\ \dot{\boldsymbol{w}} = \boldsymbol{u} \end{cases}. \tag{16}$$

Were we to have

$$\boldsymbol{w} = -\hat{\boldsymbol{D}}_f^{-1}(\boldsymbol{L} \otimes \boldsymbol{I}_m)\boldsymbol{y} - \hat{\boldsymbol{D}}_f^{-1}\dot{\boldsymbol{g}}(t) \equiv \boldsymbol{\xi}(t, \boldsymbol{y}), \tag{17}$$

the system would be stable, as proven in theorem 4. Changing the coordinates to $\boldsymbol{z} = \boldsymbol{w} - \boldsymbol{\xi}(t, \boldsymbol{y})$ leads to

$$\begin{cases} \dot{\boldsymbol{y}} = \hat{\boldsymbol{D}}_f\boldsymbol{\xi}(t, \boldsymbol{y}) + \dot{\boldsymbol{g}}(t) + \hat{\boldsymbol{D}}_f\boldsymbol{z} \\ \dot{\boldsymbol{z}} = \boldsymbol{u} - \dot{\boldsymbol{\xi}}(t, \boldsymbol{y}) \end{cases}. \tag{18}$$

Consider the candidate Lyapunov function

$$V = \frac{1}{2}\boldsymbol{y}^T\boldsymbol{y} + \frac{1}{2}\boldsymbol{z}^T\boldsymbol{z}. \tag{19}$$

Taking the derivative,

$$\dot{V} = \boldsymbol{y}^T\hat{\boldsymbol{D}}_f\boldsymbol{\xi}(t, \boldsymbol{y}) + \boldsymbol{y}^T\dot{\boldsymbol{g}}(t) + \boldsymbol{y}^T\hat{\boldsymbol{D}}_f\boldsymbol{z} + \boldsymbol{z}^T\boldsymbol{u} - \boldsymbol{z}^T\dot{\boldsymbol{\xi}}(t, \boldsymbol{y}). \tag{20}$$

Thus, making

$$\boldsymbol{u} = -\hat{\boldsymbol{D}}_f^T\boldsymbol{y} + \dot{\boldsymbol{\xi}}(t, \boldsymbol{y}) - \hat{\boldsymbol{K}}\boldsymbol{z}, \tag{21}$$

with $\hat{\boldsymbol{K}} > 0$, the derivative of the candidate Lyapunov function becomes

$$\begin{aligned} \dot{V} &= \boldsymbol{y}^T\hat{\boldsymbol{D}}_f\boldsymbol{\xi}(t, \boldsymbol{y}) + \boldsymbol{y}^T\dot{\boldsymbol{g}}(t) - \boldsymbol{z}^T\hat{\boldsymbol{K}}\boldsymbol{z} \\ &= -\boldsymbol{y}^T(\boldsymbol{L} \otimes \boldsymbol{I}_m)\boldsymbol{y} - \boldsymbol{z}^T\hat{\boldsymbol{K}}\boldsymbol{z} \end{aligned}, \tag{22}$$

which proves that the control law is stable.

Corollary 6. If $\boldsymbol{u} = \hat{\boldsymbol{K}}\hat{\boldsymbol{K}}_p^{-1}\boldsymbol{u}'$, then the control law

$$\boldsymbol{u}' = \hat{\boldsymbol{K}}_p\hat{\boldsymbol{K}}^{-1}(\dot{\boldsymbol{\xi}}(t, \boldsymbol{y}) - \hat{\boldsymbol{D}}_f^T\boldsymbol{y}) - \hat{\boldsymbol{K}}_p(\dot{\boldsymbol{x}} - \boldsymbol{\xi}(t, \boldsymbol{y})) \tag{23}$$

is stable. In particular, if the eigenvalues of $\hat{\boldsymbol{K}}$ tend to infinity, the control law becomes

$$\boldsymbol{u} = -\hat{\boldsymbol{K}}_p(\dot{\boldsymbol{x}} - \boldsymbol{\xi}(t, \boldsymbol{y})) \tag{24}$$

and all nodes converge to a consensus in $\boldsymbol{y}$.

This theorem allows the design of an outer loop to the controller that is able to connect all the vehicles to achieve a common mission. Note that, from the corollary, the control law consists of an individual derivative component followed by a global proportional component. The former may be viewed as the individual control law that the vehicles already benefit from or as an addition to said control law. This permits an independent design of the internal controller in any of the nodes, so long as they are stable on their own. This way, it is possible to separate both stages of design and/or devise a connection between already existent vehicles.

To finish this section, let's establish what are the effects of possible perturbations to the control law.

Theorem 7. Under the same notation as theorem 5, consider a strongly connected algebraic graph $G_x = (\mathcal{V}, \mathcal{E}, \boldsymbol{\mathcal{A}}, \boldsymbol{x})$ with n nodes and a corresponding Laplacian matrix $\boldsymbol{L}$. Let each value $\boldsymbol{x}_i \in \mathbb{R}^m$, with $i \in \{1, ..., n\}$ be defined by the dynamics

$$\begin{cases} \dot{\boldsymbol{x}}_i = \boldsymbol{w}_i \\ \dot{\boldsymbol{w}}_i = \boldsymbol{u}_i \\ \boldsymbol{y}_i = \boldsymbol{f}_i(\boldsymbol{x}_i) + \boldsymbol{g}_i(t) + \boldsymbol{h}_i(t) \end{cases}, \tag{25}$$

where $\boldsymbol{h}_i : \mathbb{R} \to \mathbb{R}^m$ is an unknown perturbative term. Suppose the vector $\boldsymbol{h} = [\boldsymbol{h}_1^T \ ... \ \boldsymbol{h}_n^T]^T$ satisfies

$$\|\dot{\boldsymbol{h}}(t)\| \leq \delta, \forall_{t>0}. \tag{26}$$

The control law expressed in (15) results in a bounded output when $\boldsymbol{L}$ is positive definite.

Proof. Using the candidate Lyapunov function in (19) and the control law in (15), the time derivative of the candidate function is

$$\dot{V} = -\boldsymbol{y}^T(\boldsymbol{L} \otimes \boldsymbol{I}_m)\boldsymbol{y} - \boldsymbol{z}^T\hat{\boldsymbol{K}}\boldsymbol{z} + \boldsymbol{y}^T\dot{\boldsymbol{h}}(t). \tag{27}$$

Consider the symmetric matrix defined as

$$\boldsymbol{Q}_L = \frac{1}{2}(\boldsymbol{L} \otimes \boldsymbol{I}_m + (\boldsymbol{L} \otimes \boldsymbol{I}_m)^T). \tag{28}$$

Then, letting μ_- define the smallest eigenvalue of $\boldsymbol{Q}$, which is positive because $\boldsymbol{L}$ is assumed to be positive definite, it follows from the min-max theorem, as seen in Marcus and Minc (1962), that

$$\boldsymbol{y}^T(\boldsymbol{L} \otimes \boldsymbol{I}_m)\boldsymbol{y} \geq \mu_-\|\boldsymbol{y}\|^2. \tag{29}$$

Similarly, for

$$\boldsymbol{Q}_K = \frac{1}{2}(\hat{\boldsymbol{K}} + \hat{\boldsymbol{K}}^T), \tag{30}$$

it follows that

$$\boldsymbol{z}^T\hat{\boldsymbol{K}}\boldsymbol{z} \geq \nu_-\|\boldsymbol{z}\|^2, \tag{31}$$

where ν_- is the smallest eigenvalue of $\boldsymbol{Q}_K$, which is also assumed to be positive. The derivative of the candidate Lyapunov function is thus bounded by

$$\dot{V} \leq -\mu_-\|\boldsymbol{y}\|^2 - \nu_-\|\boldsymbol{z}\|^2 + \|\boldsymbol{y}\|\|\dot{\boldsymbol{h}}(t)\|. \tag{32}$$

In turn, applying condition (26),

$$\dot{V} \leq -\mu_-\|\boldsymbol{y}\|^2 - \nu_-\|\boldsymbol{z}\|^2 + \delta\|\boldsymbol{y}\| \leq -\nu_-\|\boldsymbol{z}\|^2, \forall_{\|\boldsymbol{y}\| \geq \frac{\delta}{\mu_-}}, \tag{33}$$

which shows that $\dot{V}$ is only positive inside a ball around $\boldsymbol{y} = \boldsymbol{0}$ with radius not bigger than $\frac{\delta}{\mu_-}$, which proves that the output is bounded.

The perturbations do not compromise the stability of the system only when $\boldsymbol{L}$ doesn't have null eigenvalues, which will be true when absolute measurements are considered. As of now, only relative measurements between nodes have been established, hence why it isn't yet possible to control the value to which the nodes should reach a consensus. Logically, any perturbation will change the value of this consensus and the system cannot be stable under these conditions. In the next section, with the introduction of a reference trajectory and absolute measurements, the null eigenvalue of $\boldsymbol{L}$ disappears and the output remains bounded under bounded perturbations.

As it can be seen in the proof of the last theorem, the bounds of $\boldsymbol{y}$ become smaller with the increase of the eigenvalues of $\boldsymbol{L}$ and with the increase of the gain $\hat{\boldsymbol{K}}$, which is to be expected. However, the downside is that the system actuation becomes much more aggressive, which, in real applications, may not be ideal.

4. CONTROLLER DESIGN

Suppose we have n vehicles who communicate between each other following a strongly connected algebraic graph $G_\lambda = (\mathcal{V}, \mathcal{E}, \boldsymbol{\mathcal{A}}, \boldsymbol{\lambda})$, where $\boldsymbol{\lambda}$ represents the attitude of all considered satellites. The goal for these satellites is for them to coordinately observe points on Earth and to move accordingly as to "maintain formation".

In order to ensure the controllability of the values to which the satellites reach a consensus, imagine the presence of a "virtual" vehicle, which follows the desired trajectory perfectly and is able to inform a subset of vehicles about its current output in real time. This creates a new information graph based on the last one, $G'_\lambda = (\mathcal{V}', \mathcal{E}', \boldsymbol{\mathcal{A}}', \boldsymbol{\lambda})$, with

$$\boldsymbol{\mathcal{A}}' = \begin{bmatrix} 0 & a_{12} & ... & a_{1n} & b_1 \\ a_{21} & 0 & ... & a_{2n} & b_2 \\ \vdots & \vdots & \ddots & \vdots & \vdots \\ a_{n1} & a_{n2} & ... & 0 & b_n \\ 0 & 0 & ... & 0 & 0 \end{bmatrix}, \tag{34}$$

where the values b_i are the weights of the edges that connect the virtual vehicle to the other ones. The output error vector for the i-th vehicle may be defined as

$$\boldsymbol{\Delta y}_i = \sum_{j=1}^{n} \left(a_{ij}(\boldsymbol{y}_i - \boldsymbol{y}_j - \boldsymbol{h}_{ij}) + b_i(\boldsymbol{y}_i - \boldsymbol{y}_d - \boldsymbol{h}_{id}) \right), \tag{35}$$

where $\boldsymbol{y}_d$ is the desired output. Vectors $\boldsymbol{h}_{ij}$ represent an output offset that should exist between the i-th and the j-th vehicle, and vector h_{id} is the output offset that should exist between the i-th vehicle and the virtual vehicle. These vectors may be interpreted as the relative deviations the satellites should have amongst themselves in steady-state, in terms of the output. Concatenating these vectors into a single one, $\boldsymbol{\Delta y} = \begin{bmatrix} \boldsymbol{\Delta y}_1^T & ... & \boldsymbol{\Delta y}_n^T \end{bmatrix}^T$, leads to

$$\boldsymbol{\Delta y} = (\boldsymbol{L}' \otimes \boldsymbol{I}_3)\boldsymbol{y} - \boldsymbol{h} - (\boldsymbol{b} \otimes \boldsymbol{I}_3)\boldsymbol{y}_d \equiv \boldsymbol{L}'_3 \boldsymbol{y} - \boldsymbol{\Delta y}_{ref}. \tag{36}$$

In this equation, $\boldsymbol{L}'$ represents the Laplacian matrix of the graph G'_λ without the row and column referring to the virtual vehicle. This matrix can be constructed using the Laplacian matrix of G_λ, $\boldsymbol{L}$, by doing

$$\boldsymbol{L}' = \boldsymbol{L} + \begin{bmatrix} b_1 & ... & 0 \\ \vdots & \ddots & \vdots \\ 0 & ... & b_n \end{bmatrix}. \tag{37}$$

Finally, the vector $\boldsymbol{h}$ concatenates all the offsets for a particular vehicle, with

$$\boldsymbol{h}_i = \sum_{j=1}^{n} (a_{ij}\boldsymbol{h}_{ij} + b_i \boldsymbol{h}_{id}). \tag{38}$$

Remark 8. The null eigenvalue that was present on $\boldsymbol{L}$ by construction disappears once $\boldsymbol{L}'$ is formed.

In corollary 6, the stability of the control law (24) was proven. However, that control law acted directly on $\ddot{\boldsymbol{\lambda}}$, which isn't the case here, since the input acts on the angular velocity, which modifies the angular rates as per equation (1). Therefore, a modification of the input is required so that it acts directly on the second derivative of the Euler angles.

Let $\boldsymbol{u} = -\hat{\boldsymbol{J}}^{-1}\widehat{[\boldsymbol{\omega}_i \times]}\hat{\boldsymbol{J}}\boldsymbol{\omega} + \hat{\boldsymbol{J}}^{-1}\boldsymbol{\tau}$. The global dynamic system becomes

$$\begin{cases} \dot{\boldsymbol{\lambda}} = \hat{\boldsymbol{\Xi}}\boldsymbol{\omega} \\ \dot{\boldsymbol{\omega}} = \boldsymbol{u} \end{cases}. \tag{39}$$

In here, directly, we may add an internal feedback of the angular velocity in order to drive this state to zero and guarantee internal stability. As such, the first term of the control law should be $\boldsymbol{u}_\omega = -\hat{\boldsymbol{K}}_\omega \boldsymbol{\omega}$.

Rewriting (1) as

$$\boldsymbol{\omega} = \boldsymbol{\Xi}^{-1}\dot{\boldsymbol{\lambda}} \tag{40}$$

and taking the derivative, it follows that

$$\dot{\boldsymbol{\omega}} = \hat{\boldsymbol{\Xi}}^{-1}\ddot{\boldsymbol{\lambda}} + \frac{d\hat{\boldsymbol{\Xi}}^{-1}}{dt}\dot{\boldsymbol{\lambda}}. \tag{41}$$

Substituting the term $\ddot{\boldsymbol{\lambda}}$ with the control law (24), the outer component of the control law may be obtained as,

$$\begin{aligned} \boldsymbol{u}_y = &- \hat{\boldsymbol{\Xi}}^{-1}\hat{\boldsymbol{K}}_p\hat{\boldsymbol{D}}_f{}^{-1}(\boldsymbol{\Delta y} + \boldsymbol{v}) + \\ &+ \left(\frac{d\hat{\boldsymbol{\Xi}}^{-1}}{dt} - \hat{\boldsymbol{\Xi}}^{-1}\hat{\boldsymbol{K}}_p \right) \dot{\boldsymbol{\lambda}} \end{aligned}, \tag{42}$$

where $\boldsymbol{v} = \begin{bmatrix} \boldsymbol{v}_1^T & ... & \boldsymbol{v}_n^T \end{bmatrix}^T$, with $\boldsymbol{v}_i = [\dot{p}_{x_i} \ \dot{p}_{y_i} \ 0]^T$, represents the velocity of the satellites in reference to the $\{S\}$ frame.

Remark 9. From a direct calculation, it follows that

$$\boldsymbol{\Xi}_i^{-1} = \begin{bmatrix} \sin\theta_i \sin\psi_i & \cos\psi_i & 0 \\ \sin\theta_i \cos\psi_i & -\sin\psi_i & 0 \\ \cos\theta_i & 0 & 1 \end{bmatrix} \tag{43}$$

and, consequently,

$$\frac{d\boldsymbol{\Xi}_i^{-1}}{dt} = \begin{bmatrix} \dot{\theta}_i \cos\theta_i \sin\psi_i + \dot{\psi}_i \sin\theta_i \cos\psi_i & -\dot{\psi}_i \sin\psi_i & 0 \\ \dot{\theta}_i \cos\theta_i \cos\psi_i - \dot{\psi}_i \sin\theta_i \sin\psi_i & -\dot{\psi}_i \cos\psi_i & 0 \\ -\dot{\theta}_i \sin\theta_i & 0 & 0 \end{bmatrix}. \tag{44}$$

Furthermore, for the chosen output functions, the derivative is

$$\boldsymbol{D}_{f_i} = \begin{bmatrix} -h_i \tan\theta_i \sin\phi_i & h_i \cos\phi \sec^2\theta_i & 0 \\ h_i \tan\theta_i \cos\phi_i & h_i \sin\phi \sec^2\theta_i & 0 \\ 0 & 0 & 1 \end{bmatrix}, \tag{45}$$

which is invertible for $\theta_i \in \left]-\frac{\pi}{2}, \frac{\pi}{2}\right[/\{0\}$. Note that the singularity in 0 does not compromise stability since it is a null set, and may be treated as a special case.

Theorem 10. For the domain $\phi_i, \psi_i \in [0, 2\pi[$ and $\theta_i \in \left]-\frac{\pi}{2}, \frac{\pi}{2}\right[/\{0\}$, the control law

$$\boldsymbol{\tau} = \hat{\boldsymbol{J}}\left(\hat{\boldsymbol{J}}^{-1}\widehat{[\boldsymbol{\omega}_i\times]}\hat{\boldsymbol{J}}\boldsymbol{\omega} - \hat{\boldsymbol{K}}_\omega\boldsymbol{\omega} + \boldsymbol{u}_y\right), \tag{46}$$

with $\boldsymbol{u}_y$ defined in (42), is stable.

Remark 11. In the absence of time-dependent terms in the output equations, such as the position of the points in $\{S\}$ directly below the satellites, the control law drives the output error $\boldsymbol{\Delta y}$ to $\boldsymbol{0}$ since, from corollary 6, the control law $\boldsymbol{u}_y$ makes the output error $\boldsymbol{\Delta y}$ converge asymptotically to $\boldsymbol{0}$ because matrix $\boldsymbol{L}_3'$ does not have null eigenvalues. Furthermore, the term $-\hat{\boldsymbol{K}}_\omega\boldsymbol{\omega}$ also drives $\dot{\boldsymbol{\lambda}}$ to zero. However, taking into account the velocity of the satellites in the output equations, the damping term $-\hat{\boldsymbol{K}}_\omega\boldsymbol{\omega}$ will counteract the necessary actions that the vehicles must employ to compensate for those time-dependent components, which may result in a complete inability of the satellites to fully compensate these factors. This may result in static errors in the output.

With this result, the full controller is designed and the satellites will be able to observe the surface of the Earth with coordination. Fig. 3 represents the block diagram for this controller applied to an individual satellite.

5. SIMULATION RESULTS

5.1 Tracking performance

For the simulation, five identical satellites will be considered, each with a moment of inertia of these satellites is $\boldsymbol{J}_i = \text{diag}(700, 1100, 1300)$ kg.m^2, similar to the existing Sentinel-2, from ESA (Wiedermann et al. (2014)). The information flow between the vehicles is assumed to be as shown in Fig. 4. The objective is for the satellites to observe certain areas while they are pointing to points that form a square pattern, as shown in Fig. 5. The adjacency matrix of the information graph for this simulation will be defined as

$$\boldsymbol{\mathcal{A}} = \frac{1}{6}\begin{bmatrix} 0 & 0 & 3 & 0 & 3 \\ 0 & 0 & 3 & 0 & 3 \\ 2 & 2 & 0 & 2 & 0 \\ 0 & 0 & 3 & 0 & 3 \\ 2 & 2 & 0 & 2 & 0 \end{bmatrix} \tag{47}$$

Furthermore, only vehicle 1 will receive information about the reference trajectory, with a gain $b_1 = 1.25$.

The satellites will have circular orbits with heights $h_1 = 400$ km, $h_2 = 500$ km, $h_3 = 450$ km, $h_4 = 600$ km and $h_5 = 700$ km. The corresponding velocity magnitude is calculated using the relation

$$v_i = \sqrt{\frac{\mu_\oplus}{h_i + R_\oplus}}, \tag{48}$$

where $\mu_\oplus$ is the Earth's gravitational parameter and $R_\oplus$ is the Earth's equatorial radius. The inclinations of the orbits are $i_1 = 0°$, $i_2 = 20°$, $i_3 = 45°$, $i_4 = -20°$ and $i_5 = -45°$. Considering the flat Earth approximation and taking into account it's rotation movement, the velocities of the points directly below the satellites in $\{S\}$ are given by

$$\begin{cases} \dot{p}_{x_i} = v_i\cos(i_i) - \omega_\oplus(h_i + R_\oplus) \\ \dot{p}_{y_i} = v_i\sin(i_i) \end{cases}, \tag{49}$$

where $\omega_\oplus$ is the angular velocity of Earth's rotation. The simulation will last for 250 seconds and the orbits are defined in such a way so that all the satellites fly over the origin of S at half the simulation's time, as shown in Fig. 6.

The initial attitude will be such that the initial outputs of the satellites are

$$\begin{cases} y_{01} = \left[10 \text{ Km}, 10 \text{ Km}, 0.1 \text{ rad}\right]^T \\ y_{02} = \left[20 \text{ Km}, 30 \text{ Km}, 0 \text{ rad}\right]^T \\ y_{03} = \left[40 \text{ Km}, 50 \text{ Km}, 0.2 \text{ rad}\right]^T \\ y_{04} = \left[50 \text{ Km}, 40 \text{ Km}, -0.1 \text{ rad}\right]^T \\ y_{05} = \left[20 \text{ Km}, 20 \text{ Km}, 0.4 \text{ rad}\right]^T \end{cases}. \tag{50}$$

Every 50 seconds, the reference point that satellite 1 should be observing will be changing. Starting at point $A = (0, 0)$ km, it will change to point $B = (50, 0)$ km, then point $C = (50, 30)$ km, $D = (-40, 60)$ km and, finally, $E = (-100, -20)$ km.

As for the controller, the gains for each vehicle are $\boldsymbol{K}_{p_i} = 5\boldsymbol{I}_3$ and $\boldsymbol{K}_{\omega_i} = 0.01\boldsymbol{I}_3$.

Figures 7a, 7b and 7c show the evolution of the attitude of each vehicle throughout the simulation and the observed points in the $\{S\}$ plane throughout the simulation are shown in Fig. 8.

5.2 Performance facing perturbations

To ensure the robustness of the control law when faced with output perturbations with bounded time derivatives, some experiments will be performed with that objective in mind. Consider the same set of satellites, with the same communication graphs, the same orbits and the same control laws as in the simulations above. The output equations will be modified in order to consider unknown time dependent terms in the positions of the observed points,

$$\boldsymbol{y}_i = \begin{bmatrix} h_i\tan\theta_i\cos\phi_i + p_{x_i} + d_{x_i} \\ h_i\tan\theta_i\sin\phi_i + p_{y_i} + d_{y_i} \\ \psi_i \end{bmatrix}. \tag{51}$$

The values of $\dot{d}_{x_i}$ and $\dot{d}_{y_i}$ throughout time will be sampled from random uniform distributions bounded by -0.5 km/s and 0.5 km/s. Defining $\boldsymbol{d} = \left[\boldsymbol{d}_1^T \ ... \ \boldsymbol{d}_5^T\right]^T$, with $\boldsymbol{d}_i = \left[d_{x_i} \ d_{y_i} \ 0\right]^T$, it can be seen that

$$\|\dot{\boldsymbol{d}}\| \leq \frac{\sqrt{10}}{2}. \tag{52}$$

The communication graph considered in these simulations has a Laplacian matrix equal to

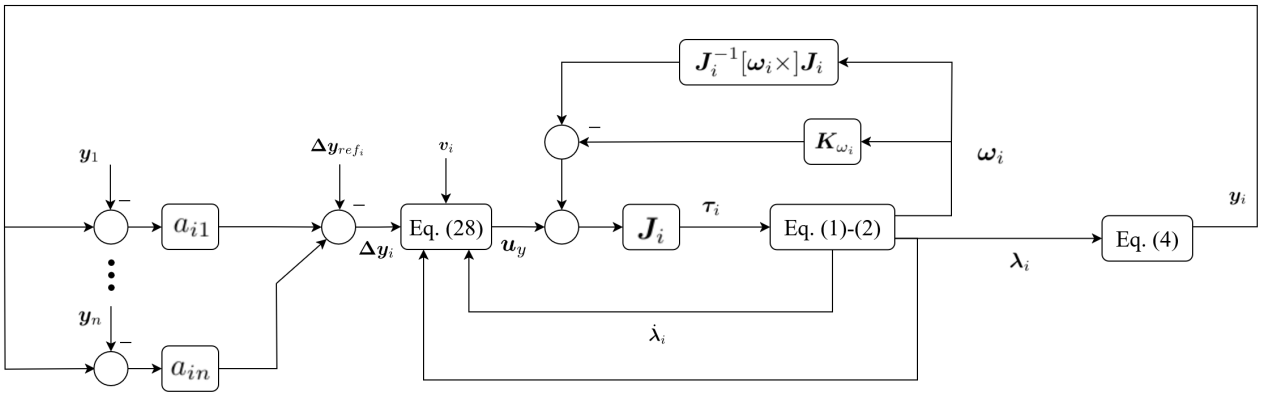

Fig. 3. Block diagram of the controller for an individual satellite

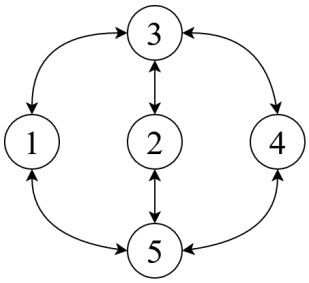

Fig. 4. Information Graph

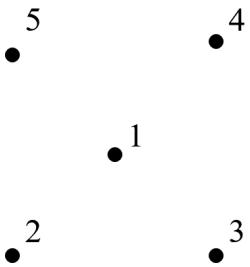

Fig. 5. Observation Pattern

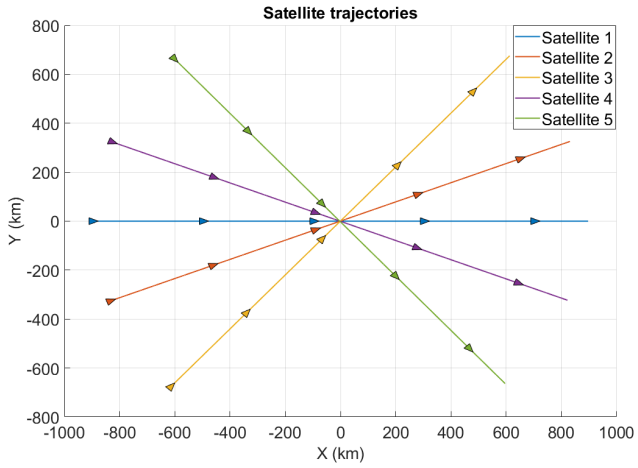

Fig. 6. Satellite trajectories on the $\{S\}$ frame

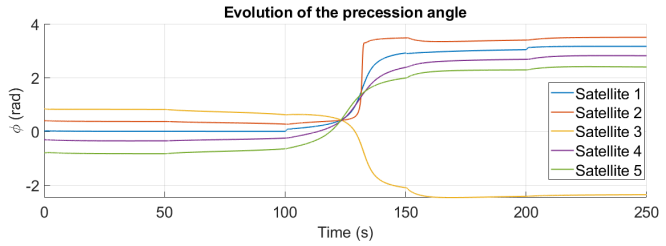

(a) Precession of the satellites

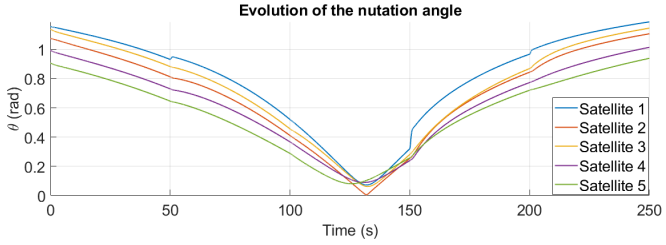

(b) Nutation of the satellites

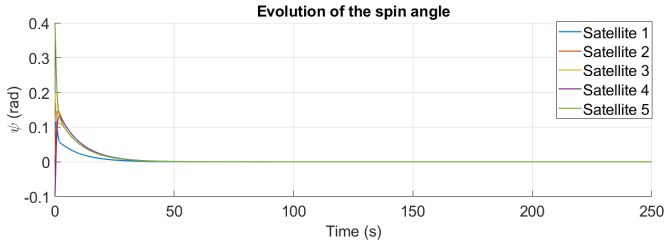

(c) Spin of the satellites

Fig. 7. Attitude of the satellites throughout the simulation

$$\boldsymbol{L}' = \frac{1}{6}\begin{bmatrix} 13.5 & 0 & -3 & 0 & -3 \\ 0 & 6 & -3 & 0 & -3 \\ -2 & -2 & 6 & -2 & 0 \\ 0 & 0 & -3 & 6 & -3 \\ -2 & -2 & 0 & -2 & 6 \end{bmatrix} \tag{53}$$

In this particular case, from (29), we have

$$\boldsymbol{y}^T(\boldsymbol{L}' \otimes \boldsymbol{I}_3)\boldsymbol{y} \geq 0.0827\|\boldsymbol{y}\|^2. \tag{54}$$

Therefore, according to (33), the observed point of each satellite should be confined to a circle of radius $\frac{\sqrt{10}}{2\times 0.0827}$ around the respective references. Figure 9 shows the simulation results with these conditions for a span of 50 seconds, assuming that the observed points by the satellites at $t = 0$ s match the reference, for simplicity of analysis. It is also represented in the plot the theoretical bounds for the position of the observed points.

5.3 Discussion of results

From Figs. 7 and 8, it can be easily seen that the control law is stable and that the satellites converge to the reference points while maintaining the desired output alignment, which, in turn, influences the states they should converge to. These convergences are smooth and without many deviations from the optimal paths between reference points. Furthermore, from inspection of Fig. 8 the static errors are minimal due to the fact that $\boldsymbol{K}_{p_i}$ is much higher than $\boldsymbol{K}_{\omega_i}$, thus, the damping term doesn't pose much of an obstacle for the compensation of satellites' orbital

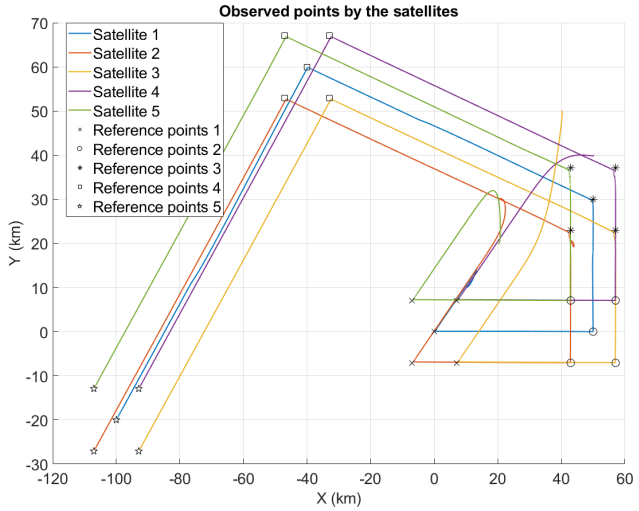

Fig. 8. Observed points in the $\{S\}$ frame

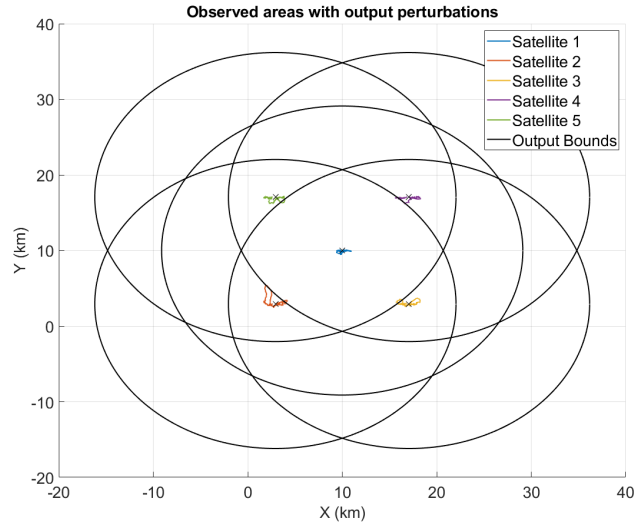

Fig. 9. Observed points in the $\{S\}$ frame with theoretical bounds for their position

velocities. The plots in Fig. 7 also show how the state of the satellites continuously changes in order to compensate the effect of the constant velocities of the satellites, resulting in a smooth tracking performance.

The performance of the controller facing output perturbations exceeds theoretical expectations, since in Fig. 9, it can be seen that the theoretical output bounds are very conservative when compared to the actual output bounds. Although these results confirm the results derived in (33), they also show that the theoretical output bounds must be refined in order to better predict what happens in reality. This may be a subject for future works on this topic.

As a final remark, by doing these simulations, one might find that the performance of the formation is as better as denser the communication graph between the vehicles is, as is to be expected. With the same logic, if the reference trajectory is known to more vehicles, then the performance further enhances. For instance, with this configuration, a compromise must be made for satellite 1 whether it should prioritize following the trajectory or to not stray much away from its peers, which naturally degrades the overall performance. The parameters that assert this compromise are the weights of the virtual satellite when constructing matrix $\boldsymbol{L}'$.

6. CONCLUSION

This article presented a non-linear distributed output tracking controller for a group of satellites, with optimal tracking performance and full consideration of the non-linear dynamics of the model. The dynamics are written in the body frame of each vehicle in order to allow the direct usage of sensor measurements and it was possible to achieve an output feedback law that ensured that the vehicles' output is properly aligned, despite them having different output equations. Simulation results were presented to experimentally confirm the results theoretically derived.

Although the proposed solution solves the stated problem successfully with satisfactory performance, it still isn't perfect and there are issues that may be subject to future works. As stated in subsection 5.3, the theoretical study on model perturbations achieved in this paper, despite being corroborated by experimental simulations, is proven to be inadequate to predict how the system behaves facing perturbations, making these theoretical output boundaries not very useful to be used in an engineering setting. Therefore, more research on how the controller behaves facing perturbations or noise would be beneficial to perfect the solution.

This has implications on other issues, namely on the subject of the flat Earth approximation considered in this paper. While this approximation may be more acceptable for Low Earth Orbit satellites, when higher orbits are considered, the mission of observing the Earth needs to take into account its curvature. This requires either a more complex output model or an assumption that the model mismatch errors are disturbances of the system that must be rejected by the controller.

The liabilities of the output equations can also be evident on the chosen method to describe the satellites' attitude. Due to the nature of the Earth observation problem, it becomes evident that the output equations are more simple and intuitive when working with the Euler sequence Z-Y-Z, as was done in this paper. However, this comes with all the problems associated with this description, such as singularities present within the working range of attitudes, namely when the nutation is null, or a highly non-linear set of dynamic equations. Other attitude description methods may overcome these issues. A different Euler sequence may place the singularities out of the reasonable range of attitudes that the satellites should achieve in this mission and quaternions may get rid of the singularities altogether and make the dynamics more easier to be handled with. However, this will inevitably make the output equations more complex, but it is still a topic that is worthy of further research.

Lastly, as was also noted, the damping terms that may be present in the preexistent controllers inside the satellites may render them unable to properly compensate the effects of their orbital velocities causing steady-state errors

in the tracking. Since these terms heighten stability, it may be unwise to simply discard them. It is hypothesized that the addition of integrative components on the control can reject the steady-state errors and increase the tracking performance. This too should be studied further.

Overall, general tools were developed that may the base of control solutions for more applications than the ones focused upon this article. While it is more intuitive to think that this may be applied to satellite formations composed of vehicles near to each other, in reality, there is not much of a limit of how different the satellites must be or how different their orbits are. It is possible, for instance, to have satellites designed for individual missions, but temporarily cooperate with each other if they are sufficiently close.

Much more can be perfected which indicates that there is more to be investigated following this work. These possible future findings may be subject for subsequent articles and contributions to a much better tool that might bring very interesting applications.

ACKNOWLEDGEMENTS

The authors acknowledge the Portuguese Foundation for Science and Technology (FCT) for its financial support via the projects LAETA Base Funding
(DOI: 10.54499/UIDB/50022/2020).

REFERENCES

Abdessameud, A. and Tayebi, A. (2008). Attitude synchronization of a spacecraft formation without velocity measurement. *47th IEEE Conference on Decision and Control*, 3719–3724. doi:10.1109/CDC.2008.4738745.

Alvarez, J. and Walls, B. (2016). Constellations, clusters, and communication technology: Expanding small satellite access to space. *2016 IEEE Aerospace Conference*, 1–11. doi:10.1109/AERO.2016.7500896.

Fax, J.A. and Murray, R.M. (2004). Information flow and cooperative control of vehicle formations. *IEEE Transactions on Automatic Control*, 49(9), 1456–1476. doi:10.1109/TAC.2004.834433.

Khalil, H. (2001). *Nonlinear Systems*. Pearson, Michigan.

Lawton, J.R. and Beard, R.W. (2002). Synchronized multiple spacecraft rotations. *Automatica*, 8, 1359–1364. doi:10.1016/S0005-1098(02)00025-0.

Marcus, M. and Minc, H. (1962). *A Survey of Matrix Theory and Matrix Inequalities*. Allyn and Bacon, Michigan.

Olfati-Saber, R., Fax, J.A., and Murray, R.M. (2007). Consensus and cooperation in networked multi-agent systems. *Proceedings of the IEEE*, 95(1), 215–233. doi: 10.1109/JPROC.2006.887293.

Olfati-Saber, R. and Murray, R.M. (2004). Consensus problems in networks of agents with switching topology and time-delays. *IEEE Transactions on Automatic Control*, 49, 1520–1533. doi:10.1109/TAC.2004.834113.

Ren, W. (2002). Distributed attitude alignment in spacecraft formation flying. 21, 95–113. doi:10.1002/acs.916.

Wiedermann, G., Gockel, W., Winkler, S., Rieber, J.M., Kraft, B., and Reggio, D. (2014). The sentinel-2 satellite attitude control system - challenges and solutions. *9th International ESA Conference on Guidance, Navigation and Control Systems*.

Wu, Q., Hou, T., Shi, L., and Li, Y. (2020a). Robust consensus of multi-satellite systems based on the characteristic model method. *2020 IEEE 16th International Conference on Control and Automation (ICCA)*, 153–158. doi:10.1109/ICCA51439.2020.9264529.

Wu, Q., Hou, T., Shi, L., and Li, Y. (2020b). Semi-global output consensus of multi-satellite systems based on characteristic model method with disturbance and actuator saturation. *2020 Chinese Automation Congress (CAC)*, 6197–6202. doi: 10.1109/CAC51589.2020.9327885.

Ziyang, M., You, Z., Guanhua, L., and Chunshi, F. (2010). Cooperative attitude control of multiple rigid bodies with multiple time-varying delays and dynamically changing topologies. *Mathematical Problems in Engineering*, 2010. doi:10.1155/2010/621594.